

# Solar photocatalytic decolorization of C.I. Basic Blue 41 in an aqueous suspension of TiO<sub>2</sub>–ZnO

Yinhua Jiang<sup>a,b</sup>, Yueming Sun<sup>a,\*</sup>, Hui Liu<sup>a,b</sup>, Fuhong Zhu<sup>b</sup>, Hengbo Yin<sup>b</sup>

<sup>a</sup> School of Chemistry and Chemical Engineering, Southeast University, Nanjing 210096, PR China

<sup>b</sup> School of Chemistry and Chemical Engineering, Jiangsu University, Zhenjiang 212013, PR China

Received 17 August 2007; received in revised form 19 October 2007; accepted 24 October 2007

Available online 5 November 2007

## Abstract

Nanosized, bicomponent TiO<sub>2</sub>–ZnO powders of varying Ti/Zn ratio, were prepared using an ultrasonic precipitation method and their crystalline structure and surface area were determined using X-ray diffraction and N<sub>2</sub> physical adsorption. The nanosized TiO<sub>2</sub>–ZnO powders displayed high photocatalytic activity towards the decolorization of C.I. Basic Blue 41 in water under solar irradiation and a Ti/Zn molar ratio of 1:1 showed highest photocatalytic activity. The effects of various parameters such as photocatalyst loading, initial solution pH, initial dye concentration and irradiation time on decolorization rate were systematically investigated. The optimal TiO<sub>2</sub>–ZnO concentration range was around 6–10 g/L. Optimal pH was ~6.21 which was the natural pH of a 20 mg/L aqueous solution of the dye. Approximately 100% color removal was achieved in about 1 h; the addition of a surfactant and an antistatic agent hindered photocatalytic decolorization, which obeyed pseudo-first-order kinetics.

© 2007 Elsevier Ltd. All rights reserved.

**Keywords:** Nanosized TiO<sub>2</sub>–ZnO; Photocatalyst; C.I. Basic Blue 41; Solar photocatalytic decolorization

## 1. Introduction

Dyes widely used in textiles, paper, rubber and plastics industries often create severe environmental pollutions in the form of colored wastewater discharged into environmental water bodies. It affects aesthetic merit, and reduces light penetration and photosynthesis. In addition, some dyes are either toxic or mutagenic and carcinogenic [1]. The conventional methods for treating dye-containing wastewaters are usually ineffective in removal of these compounds or just transfer the contamination from one phase to another [2]. Biodegradation of dyes may be selective, incomplete, and some dyes with aromatic structure are difficult to biodegrade [3]. Moreover, some biodegradation products are even more toxic than the degraded dye [4].

A promising method as an alternative to conventional methods for dye degradation is represented by the semiconductor photocatalysis, which has already been used successfully for the destruction of a great variety of organic compounds [5–14]. A variety of semiconductor powders such as TiO<sub>2</sub>, ZnO, WO<sub>3</sub> and so on, acting as photocatalysts, have been used in the semiconductor photocatalysis. Among these semiconductors, TiO<sub>2</sub> has been extensively investigated as the most promising photocatalyst due to its high photocatalytic activity, non-toxicity, high photochemical stability and low-cost. However, TiO<sub>2</sub> can only absorb a small portion of solar spectrum in the UV region [15] and has high recombination rate of photo-induced electron–hole pairs at or near its surface [16]. Solar energy, an abundant natural energy source, has been successfully used for photocatalytic degradation of pollutants [17,18]. In order to make TiO<sub>2</sub> suitable for receiving and utilizing solar energy with good efficiency, many methods such as dye sensitization, metal or nonmetal doped TiO<sub>2</sub>-based nanoparticles and modification of TiO<sub>2</sub> by addition of another semiconductor have been used to improve the photocatalytic

\* Corresponding author. Tel.: +86 25 52084679; fax: +86 25 52090621.  
E-mail address: [jyinhua@126.com](mailto:jyinhua@126.com) (Y. Sun).

properties of titanium dioxide. It has been shown that coupled semiconductor seems to be a simple and viable method. Photocatalytic process is based on the generation of electron–hole pairs by means of band-gap radiation that can give rise to redox reactions with the species adsorbed on the surface of the photocatalysts. In principle, the coupling of different semiconductor oxides seems useful in order to achieve a more efficient electron–hole pair separation under irradiation and, consequently, a higher photocatalytic activity [19]. Various composites formed by  $\text{TiO}_2$  and other inorganic oxides or sulfides such as  $\text{SiO}_2$  [5],  $\text{SnO}_2$  [6],  $\text{Cu}_2\text{O}$  [7],  $\text{MgO}$  [8],  $\text{WO}_3$  [9],  $\text{In}_2\text{O}_3$  [10],  $\text{ZnO}$  [11],  $\text{MoO}_3$  [12],  $\text{CdS}$  [13],  $\text{PbS}$  [14] and so on, have been reported.

It is well known that  $\text{ZnO}$  is a suitable alternative to  $\text{TiO}_2$  because its photodegradation mechanism has been proven to be similar to that of  $\text{TiO}_2$ , and in fact higher photocatalytic efficiency compared with  $\text{TiO}_2$  has been reported for  $\text{ZnO}$  [20,21]. The biggest advantage of  $\text{ZnO}$  is that it can absorb over a larger fraction of UV spectrum and the corresponding threshold of  $\text{ZnO}$  is 425 nm [22]. In this paper, nanosized bicomponent  $\text{TiO}_2$ – $\text{ZnO}$  photocatalysts were prepared by ultrasonic precipitation followed by heat treatment starting from low-cost metatitanic acid. The properties of the bicomponent oxides were studied by X-ray diffraction (XRD) and  $\text{N}_2$  adsorption technique. Subsequent experiments were conducted to investigate the effects of various process variables on the process of the photodecolorization of C.I. Basic Blue 41, under solar irradiation using  $\text{TiO}_2$ – $\text{ZnO}$  powder as a photocatalyst. C.I. Basic Blue 41, a monoazo-basic dye of bright blue hue, was chosen as a model dye because it is widely used in textile industry and cannot be quickly degraded. Structure of C.I. Basic Blue 41 is given in Fig. 1.

## 2. Experimental

### 2.1. Materials

Metatitanic acid ( $\text{H}_2\text{TiO}_3$ ) containing 2 wt% of anatase crystal seeds with particle sizes in the range of 2–5 nm was supplied by Jiangsu Titanium Dioxide Pigment Company, China. Concentrated sulfuric acid (98%), zinc acetate dehydrate, sodium hydroxide, and ethanol of analytical reagent grade were purchased from Shanghai Chemical Reagent Company, China. Distilled water was used throughout in all the experiments. C.I. Basic Blue 41 (purity  $\geq 98\%$ ) was the commercial product supplied by the dye company and used without further purification.

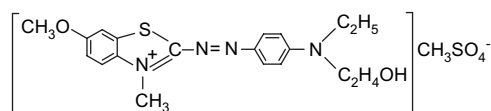


Fig. 1. The structure of C.I. Basic Blue 41.

### 2.2. Preparation and characterization of nanosized $\text{TiO}_2$ – $\text{ZnO}$ photocatalyst

For preparation of nanosized  $\text{TiO}_2$ – $\text{ZnO}$  photocatalysts (samples 2–6), the required amount of metatitanic acid was dispersed in 20 mL of distilled water and sonicated in an ultrasonic bath under 30 kHz frequency for 15 min. Then metatitanic acid suspension was added into 30 mL of  $\text{Zn}(\text{CH}_3\text{COO})_2$  (0.5 mol/L) aqueous solution, in which the additive amount of metatitanic acid was determined by Ti/Zn molar ratio ranging from 4:1 to 0:1. Prepared suspension was again sonicated for 15 min in order to improve the dispersion of metatitanic acid in  $\text{Zn}(\text{CH}_3\text{COO})_2$  aqueous solution. Then 60 mL of  $\text{NaOH}$  (0.5 mol/L) aqueous solution was added dropwise into the above suspension under ultrasonic agitation so as to obtain  $\text{Zn}(\text{OH})_2$  precipitation. After the completion of the reaction, the mixed suspension was further sonicated for 15 min and filtered. The resulting solids were washed with distilled water and ethanol for several times. Then the precursors were dried at 80 °C for 3–4 h and calcined at 300 °C for 2 h. A series of nanosized  $\text{TiO}_2$ – $\text{ZnO}$  photocatalysts, in which the zinc concentration was different, were prepared. Pure  $\text{TiO}_2$  (sample 1, Ti/Zn = 1:0) was also prepared by the above method only without adding  $\text{Zn}(\text{CH}_3\text{COO})_2$  and  $\text{NaOH}$  solution.

The chemical structures of the as-prepared samples were characterized by powder X-ray diffraction (XRD) on a Rigaku D-max 2200 X-ray diffractometer with  $\text{Cu K}\alpha$  radiation ( $\lambda = 1.5406 \text{ \AA}$ ). The specific surface area (BET) was estimated from the  $\text{N}_2$  adsorption/desorption isotherms, measured by a Quantachrome NOVA2000 surface area apparatus.

### 2.3. Photocatalysis studies

Photocatalytic experiments were carried out in a 100 mL capacity borosilicate photochemical batch reactor with dimensions  $8 \times 4 \text{ cm}$  (height  $\times$  diameter). All photocatalytic experiments were carried out under the similar conditions on sunny days of April–May between 10 A.M. and 2 P.M. when the solar intensity fluctuations were minimal. A series of 20 mg/L C.I. Basic Blue 41 solutions were prepared. The pH of dye solutions were adjusted to desired level using dilute  $\text{NaOH}$  and  $\text{H}_2\text{SO}_4$ . Reaction suspension was prepared by adding appropriate quantity of photocatalyst into 50 mL of C.I. Basic Blue 41 aqueous solutions and magnetically stirred in dark for 30 min to establish adsorption–desorption equilibrium. The suspension containing C.I. Basic Blue 41 and photocatalyst was then irradiated under the sunlight, and the photocatalytic reaction timing was started. During the experiment, the reaction mixture was stirred vigorously using magnetic stirrer. The reaction mixture was withdrawn after an appropriate irradiation time, centrifuged at 8000 rpm to remove any suspended solids and analyzed by a TU-1201 UV–vis spectrophotometer at  $\lambda_{\text{max}} = 606 \text{ nm}$  for the concentration of the remaining dye in the solution. The decolorization efficiency was observed in terms of change in intensity at  $\lambda_{\text{max}}$  of the dyes. The decolorization

efficiency ( $D$ ) was calculated as  $D = ([\text{dye}]_0 - [\text{dye}]) / [\text{dye}]_0 \times 100\%$ , where  $[\text{dye}]_0$  was the equilibrium concentration of C.I. Basic Blue 41 after adsorption–desorption equilibrium, and  $[\text{dye}]$  was the concentration of C.I. Basic Blue 41 at solar irradiation time “ $t$ ”.

### 3. Results and discussion

#### 3.1. Characterization of nanosized $\text{TiO}_2$ – $\text{ZnO}$ photocatalysts

Fig. 2 shows XRD patterns of prepared samples 1–6. From the XRD patterns and the corresponding characteristic  $2\theta$  values of the diffraction peaks, it can be confirmed that  $\text{TiO}_2$  in as-prepared samples is identified as anatase-phase (PDF# 21-1272), while  $\text{ZnO}$  is zincite-phase (PDF# 36-1451). No other polymorph of titania is observed. In Fig. 2, the data also show that the molar ratio of  $\text{Ti}/\text{Zn}$  has a great influence on the phase composition. When the XRD pattern of sample with  $\text{Ti}/\text{Zn}$  molar ratio of 4:1 is compared with PDF# 21-1272 data files, it can be found that all the sharp peaks belong to anatase- $\text{TiO}_2$ , and peaks corresponding to  $\text{ZnO}$  are not detected. The possible reason is that microcrystal of  $\text{ZnO}$  is widely dispersed on the surface of  $\text{TiO}_2$  due to the small amount of  $\text{ZnO}$  and the huge surface area of  $\text{TiO}_2$ . As the  $\text{Ti}/\text{Zn}$  molar ratio decreased, the diffraction peaks of  $\text{ZnO}$  are detected and continuously getting sharper. The phases of the photocatalyst with the  $\text{Ti}/\text{Zn}$  molar ratio of 1:1 are the couple of  $\text{TiO}_2$  and  $\text{ZnO}$ .

Average crystallite size of  $\text{TiO}_2$ – $\text{ZnO}$  photocatalyst was estimated according to Scherrer's equation [23],  $d = k\lambda / (\beta \cos(2\theta))$ , where  $d$  was the average crystallite size (nm),  $\lambda$  was the wavelength of the Cu  $K\alpha$  applied ( $\lambda = 0.15406$  nm),  $\theta$  was the Bragg's angle of diffraction,  $\beta$  was the full-width at half maximum intensity of the peak and  $k$  was the constant usually applied as 0.89. The average crystallite size of  $\text{TiO}_2$ – $\text{ZnO}$  photocatalyst with  $\text{Ti}/\text{Zn}$  molar ratio of 1:1 was estimated to be 44.1 nm. The specific surface area of  $\text{TiO}_2$ – $\text{ZnO}$  photocatalyst was calculated as  $124.85 \text{ m}^2/\text{g}$  using the BET method, and with average pore sizes of 3.42 nm.

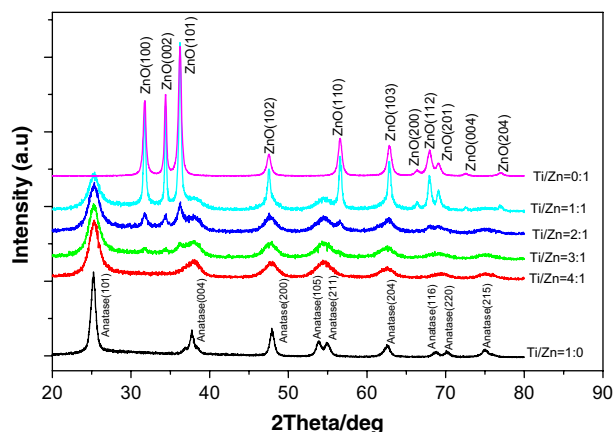


Fig. 2. X-ray diffraction (XRD) patterns of samples 1–6.

#### 3.2. Effect of $\text{Ti}/\text{Zn}$ molar ratio on the photocatalytic activity of $\text{TiO}_2$ – $\text{ZnO}$

In order to elucidate the effect of the  $\text{Ti}/\text{Zn}$  molar ratio on the photocatalytic activity of  $\text{TiO}_2$ – $\text{ZnO}$  photocatalyst, a set of parallel experiments were conducted with samples 1–6. Fig. 3 shows the effect of  $\text{Ti}/\text{Zn}$  molar ratio on the photodecolorization of C.I. Basic Blue 41. As seen from Fig. 3,  $\text{TiO}_2/\text{ZnO}$  composite nanoparticles (samples 2–5) had a higher photocatalytic activity, which was represented by larger decolorization efficiency, than pure  $\text{TiO}_2$  (sample 1).  $\text{TiO}_2/\text{ZnO}$  composite nanoparticles except sample 2 also showed a higher photocatalytic activity than pure  $\text{ZnO}$  (sample 6) and sample 5 with the  $\text{Ti}/\text{Zn}$  molar ratio of 1:1 is a superior catalyst with the decolorization efficiency of 99.16%. The highest photocatalytic activity of  $\text{TiO}_2/\text{ZnO}$  composite nanoparticles with the  $\text{Ti}/\text{Zn}$  molar ratio of 1:1 is related to the role of  $\text{ZnO}$  on the surface of  $\text{TiO}_2$  nanoparticles. In the  $\text{TiO}_2/\text{ZnO}$  composite, the electron transfer occurs from the conduction band of light-activated  $\text{ZnO}$  to the conduction band of light-activated  $\text{TiO}_2$  and, conversely, hole transfer can take place from the valence band of  $\text{TiO}_2$  to the valence band of  $\text{ZnO}$  [24,25]. This efficient charge separation increases the photocatalytic activity of  $\text{TiO}_2/\text{ZnO}$  composite. Furthermore, the highest photocatalytic activity may also be related to the amount of  $\text{ZnO}$ , which has to be sufficient to trap the photogenerated electrons. As for sample 2, the effect of photogenerated electron trapped by  $\text{ZnO}$  was not obvious because of the insufficiency of  $\text{ZnO}$ , so its photocatalytic activity was a little lower than that of samples 3–5. Thus, all further studies were carried out using the sample in  $\text{Ti}/\text{Zn}$  molar ratio of 1:1 as a photocatalyst.

#### 3.3. Effect of photocatalyst loading

In order to avoid the use of excess catalyst, it is necessary to find out the optimum loading for efficient removal of the dye. A series of experiments were carried out by varying

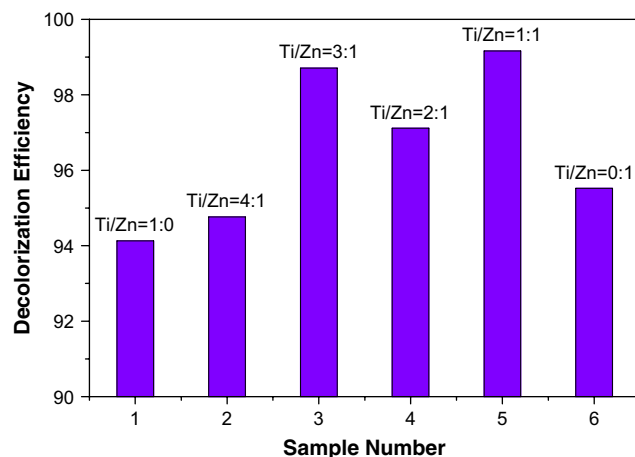


Fig. 3. The effect of samples 1–6 on decolorization efficiency of C.I. Basic Blue 41 (dye concentration 20 mg/L; catalyst dose 10 g/L; solution pH 6.21; solar irradiation time 1 h).

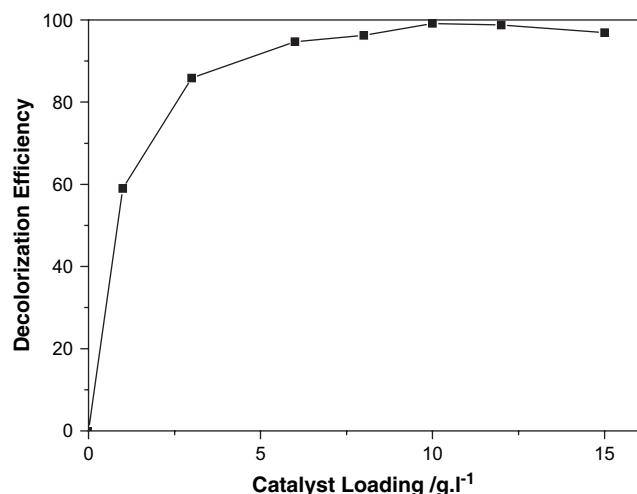


Fig. 4. Effect of nanosized  $\text{TiO}_2\text{--ZnO}$  loading on decolorization efficiency of C.I. Basic Blue 41.

the amount of catalyst from 0 to 15 g/L with the dye concentration of 20 mg/L, solution pH of 6.21 and solar irradiation time of 1 h. The decolorization efficiency of C.I. Basic Blue 41 for various photocatalyst loadings has been depicted in Fig. 4. As seen, a negligible decolorization efficiency of C.I. Basic Blue 41 with the solar light in the absence of catalyst is observed, which indicates that the dye is resistant to self-photolysis in the solar light. Fig. 4 also clearly shows that the increase in the catalyst weight from 1 to 6 g/L increases the dye decolorization sharply from 58.98 to 94.72%. This is due to the increasing photocatalyst dosage causing an increase in availability of active sites on the catalyst surface, which in turn, increases the number of photons absorbed and the number of dye molecules adsorbed, and as a result increases the decolorization rate. With increase of the catalyst loading from 6 to 10 g/L, the decolorization rate is almost constant, which suggests that an optimal level for catalyst effectiveness exists. With the increase of the catalyst loading beyond 10 g/L a slow decrease in decolorization rate of C.I. Basic Blue 41 is observed. This phenomenon may be due to the hindrance and blocking of light penetration caused by the excessive amount of  $\text{TiO}_2\text{--ZnO}$  particles [26]. On the other hand, at high concentrations of catalysts, particle aggregation may also reduce the catalytic activity. So the optimal amount range of catalyst was 6–10 g/L with dye concentration of 20 mg/L. Since the maximum decolorization of C.I. Basic Blue 41 was observed with 10 g/L of  $\text{TiO}_2\text{--ZnO}$  nanopowder, the other experiments were performed in this concentration.

### 3.4. Effect of pH

The influence of the initial pH of the dye solution was studied in the pH range 1.0–7.0 (dye concentration = 20 mg/L, catalyst loading = 10 g/L, solar irradiation time = 1 h) since pH could be considered as one of the most important parameters that could affect the photo-oxidation process [27].

Fig. 5 shows the color removal efficiency of C.I. Basic Blue 41 as a function of pH. The decolorization efficiency in the first stage increases rapidly with the increasing pH from 1.0 to 3.0, but at pH = 4 there is a slight decrease of the decolorization rate. Thereafter, the decolorization efficiency increases with the increasing pH from 4.0 to 6.21, and the maximum photodecolorization rate is at pH 6.21, which is the natural pH of the 20 mg/L aqueous solution of C.I. Basic Blue 41 without controlling, and further increase in pH causes a decrease in the decolorization rate. The pH effect on the photodecolorization of dye in the presence of  $\text{TiO}_2\text{--ZnO}$  can be explained on the basis of the point of zero charge ( $\text{pH}_{\text{zpc}}$ ) of  $\text{TiO}_2\text{--ZnO}$  particle [5,28]. So at lower pH the surface of the catalyst is positively charged, but at higher pH it becomes negatively charged. Since C.I. Basic Blue 41 is a cationic dye, high pH favors adsorption on the catalyst surface which results in high decolorization efficiency. However, C.I. Basic Blue 41 is not stable at strong alkaline condition. On the other hand, at low pH the photocorrosion of ZnO [29] may take place. As a result, the optimal operational pH was 6.21 during these experiments.

### 3.5. Effect of initial dye concentration

The initial dye concentration is a very important parameter in wastewater treatment. The effect of initial dye concentration on the decolorization efficiency was investigated by varying the dye concentrations from 20 to 100 mg/L at its natural pH with the constant catalyst loading 10 g/L. The results are shown in Fig. 6. It can be seen that with the increasing initial dye concentration, the decolorization efficiency of C.I. Basic Blue 41 decreases. Similar results are also obtained in other studies for the photocatalytic oxidation of other dyes [30–32]. As the initial concentration of dye increases, the color of dye solution becomes deeper and deeper resulting in the reduction of the penetration of light to the surface of the catalyst. The increase in dye concentration also decreases

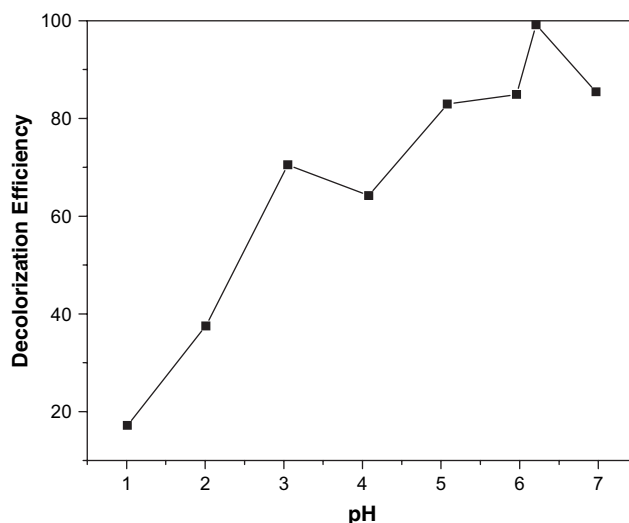


Fig. 5. Effect of pH on decolorization efficiency of C.I. Basic Blue 41.

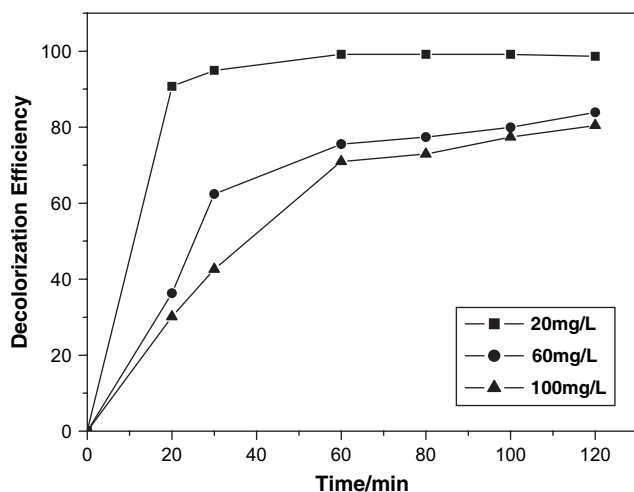


Fig. 6. Effect of the initial dye concentration on the decolorization efficiency.

the concentration of OH radical on the surface of catalyst since the active sites are occupied by the dye ions. Consequently, the decolorization percentage of the dye decreases as the dye concentration increases.

Several experimental results [18,30] indicate that heterogeneous photocatalytic decolorization and degradation of various dyes are well described by a pseudo-first-order kinetic for diluted solutions. The photocatalytic decolorization of C.I. Basic Blue 41 containing  $\text{TiO}_2\text{--ZnO}$  obeys pseudo-first-order kinetics. At low initial dye concentration the rate expression is given by

$$-\frac{d[\text{dye}]}{dt} = k_{\text{app}}[\text{dye}] \quad (1)$$

The integration of Eq. (1) is given by

$$\ln\left(\frac{[\text{dye}]_0}{[\text{dye}]}\right) = k_{\text{app}}t \quad (2)$$

where  $k_{\text{app}}$  is the pseudo-first-order rate constant.  $[\text{dye}]_0$  is the equilibrium concentration of the C.I. Basic Blue 41 solution after adsorption and it is taken as the concentration of dye solution at solar irradiation time “ $t = 0$ ” for kinetic analysis.  $[\text{dye}]$  is the concentration of C.I. Basic Blue 41 at solar irradiation time “ $t$ ” and “ $t$ ” is the solar irradiation time (min).

A plot of  $\ln([\text{dye}]_0/[\text{dye}])$  versus solar irradiation time for the C.I. Basic Blue 41 photodecolorization catalyzed by  $\text{TiO}_2\text{--ZnO}$  is shown in Fig. 7. A linear relation between dye concentration and solar irradiation time has been observed. When the initial dye concentration changes from 20 to 100 mg/L, the correlation constant for the fitted line is calculated to be  $R^2 = 0.96389$ ,  $0.99855$  and  $0.94226$ , respectively. The pseudo-first-order rate constants are calculated to be  $0.08256$ ,  $0.02369$  and  $0.01850 \text{ min}^{-1}$ , which decrease as the initial reactant concentration increases. This can be ascribed to the decrease in the number of active sites on the catalyst surface due to the covering of the surface with dye molecules, which

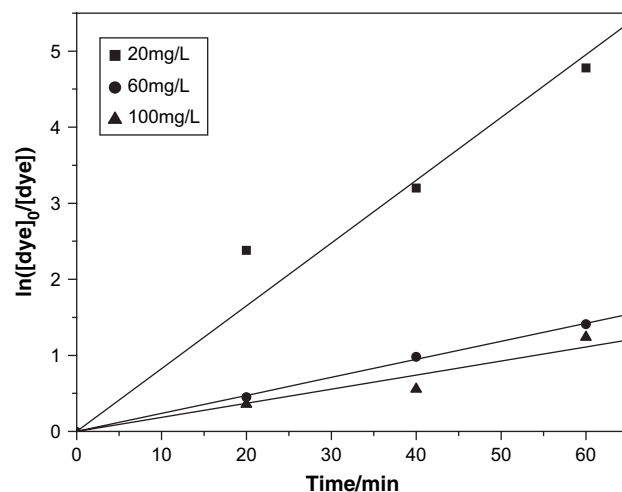


Fig. 7. Kinetics of C.I. Basic Blue 41 decolorization for different initial concentrations.

is directly proportional to the initial concentration of C.I. Basic Blue 41.

### 3.6. UV–vis spectrum

According to Fig. 4, the aqueous solutions of C.I. Basic Blue 41 are fairly stable to solar irradiation in the absence of nanosized  $\text{TiO}_2\text{--ZnO}$ . However, C.I. Basic Blue 41 can be decolorized efficiently in aqueous  $\text{TiO}_2\text{--ZnO}$  dispersions by solar light irradiation. The progress in the absorbance spectra of the dye solution during the reaction was monitored with initial 20 mg/L dye concentration and 10 g/L catalyst loading at pH 6.21. Results are shown in Fig. 8. As seen, C.I. Basic Blue 41 shows a maximum absorption peak at 606 nm and the decolorization efficiency is recorded with respect to the change in intensity of absorption peaks at 606 nm. During solar irradiation, the characteristic absorption peaks of the dye around 606 nm decreased rapidly with no

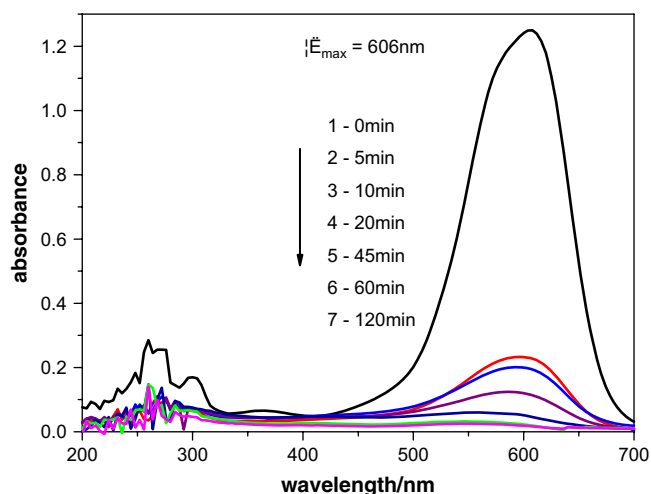


Fig. 8. Typical absorbance spectra of the dye solution during the course of the reaction, at times: (1) 0, (2) 5, (3) 10, (4) 20, (5) 45, (6) 60 and (7) 120 min.



hypsochromic shifts and no new absorption bands appeared even in the ultraviolet range ( $\lambda > 200$  nm). It may indicate a rapid degradation of C.I. Basic Blue 41, and the photodegradation mechanism may be favorable to the cleavage of the whole conjugated chromophore structure of the dye. On the other hand, the decrease in the absorbance under 300 nm is also a strong indication of the degradation of dye. After solar irradiation for 1 h, the maximum absorption peaks around 606 nm disappeared completely; however, small absorbance peaks under 300 nm still could be observed. It is clear that a total degradation of dye needs a longer reaction time than 60 min, which may be sufficient for a successful decolorization process.

### 3.7. Effect of the additives

Some dyeing additives are often used in the dyeing process, such as surfactant and antistatic agent. Therefore, the dye industry wastewater contains a considerable amount of surfactant or antistatic agent. Surfactant 1227 and antistatic agent SN are the most common additives in the cationic dyeing process; hence, it is important to study the influence of surfactant 1227 and antistatic agent SN in the photodecolorization of C.I. Basic Blue 41. The structures of surfactant 1227 and antistatic agent SN are given in Fig. 9.

Four groups of controlled experiments were carried out under the following conditions (dye concentration = 20 mg/L, catalyst loading = 10 g/L, solar irradiation time = 1 h): (i) dye solution without any additives; (ii) dye solution with 10 drops of antistatic agent SN; (iii) dye solution with 10 drops of surfactant 1227; (iv) dye solution with 5 drops of surfactant 1227 and 5 drops of antistatic agent SN. The results are shown in Fig. 10. The addition of surfactant 1227 and antistatic agent SN inhibits the photocatalytic decolorization of C.I. Basic Blue 41. The retarding effect of surfactant 1227 and antistatic agent SN in this system can be explained by competitive absorption on the surface of  $\text{TiO}_2\text{--ZnO}$  catalyst with C.I. Basic Blue 41 and surfactant 1227 or antistatic agent SN due to their similar structures. On the other hand, surfactant 1227 or antistatic agent SN can also be photodegraded by semiconductor metal oxide catalysts [33]. As a result, the decolorization efficiency of C.I. Basic Blue 41 decreased.

## 4. Conclusion

In this study, the feasibility of photocatalytic decolorization and degradation of C.I. Basic Blue 41 using nanosized  $\text{TiO}_2\text{--ZnO}$  as a photocatalyst in the form of suspension by

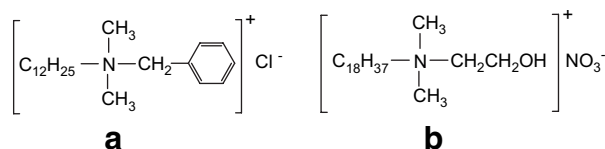


Fig. 9. (a) Structure of surfactant 1227 and (b) structure of antistatic agent SN.

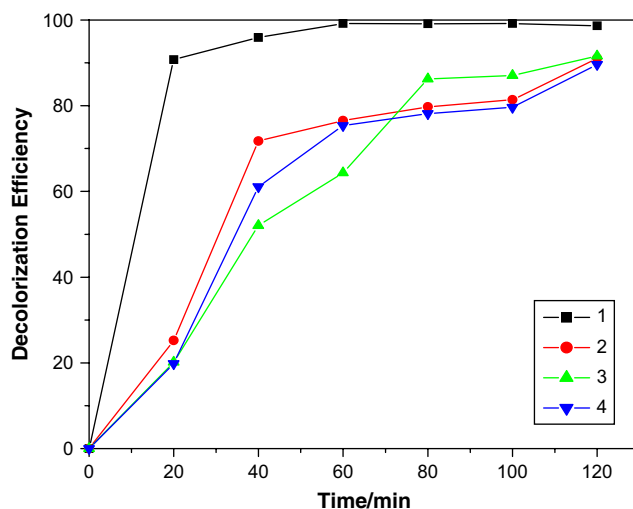


Fig. 10. Effect of additives on the decolorization efficiency of C.I. Basic Blue 41: (1) dye solution without any additives, (2) dye solution with antistatic agent SN, (3) dye solution with surfactant 1227, and (4) dye solution with antistatic agent SN and surfactant 1227.

irradiation with solar light has been shown. The experimental results demonstrated that nanosized  $\text{TiO}_2\text{--ZnO}$  with Ti/Zn molar ratio of 1:1 was the most active photocatalyst and the dye was resistant to self-photolysis in solar light. The results also indicated that decolorization efficiency of C.I. Basic Blue 41 was obviously affected by solar irradiation time, solution pH, initial dye concentration and catalyst amount. The optimal amount range of catalyst was 6–10 g/L with dye concentration of 20 mg/L. The optimal operational pH was 6.21, which was at the natural pH of the dye solution. Nearly 100% color removal, after selection of optimal operational parameters, could be achieved in a relatively short solar irradiation time of about 1 h. The additives such as surfactant 1227 and antistatic agent SN hindered the photocatalytic decolorization of dye. The photocatalytic decolorization of C.I. Basic Blue 41 containing  $\text{TiO}_2\text{--ZnO}$  obeyed pseudo-first-order kinetics model.

## Acknowledgements

The support of this research by the Doctoral Program Foundation of Higher Education (20030286012) and the High-Technique Project Foundation of Jiangsu Province (200470 and BG 2005034) is gratefully acknowledged.

## References

- [1] Gong RM, Li M, Yang C, Sun YZ, Chen J. Removal of cationic dyes from aqueous solution by adsorption on peanut hull. *J Hazard Mater B* 2005;121:247–50.
- [2] Daneshvar N, Salari D, Khataee AR. Photocatalytic degradation of azo dye Acid Red 14 in water on ZnO as an alternative catalyst to  $\text{TiO}_2$ . *J Photochem Photobiol A Chem* 2004;162:317–22.
- [3] Mozia S, Tomaszewska M, Kosowska B, Grzmil B, Morawski AW, Kalucki K. Decomposition of nonionic surfactant on a nitrogen-doped photocatalyst under visible-light irradiation. *Appl Catal B Environ* 2005;55:195–200.

- [4] Mohn WW, Martin VJJE, Yu ZT. Treatment of bleaching effluent in sequential activated sludge and nitrification systems. *Water Sci Technol* 1999;40:269–74.
- [5] Hu C, Tang YC, Yu JC, Wong PK. Photocatalytic degradation of Cationic Blue X-GRL adsorbed on  $\text{TiO}_2/\text{SiO}_2$  photocatalyst. *Appl Catal B Environ* 2003;40:131–40.
- [6] Yang J, Li D, Wang X, Yang XJ, Lu LD. Rapid synthesis of nanocrystalline  $\text{TiO}_2/\text{SnO}_2$  binary oxides and their photoinduced decomposition of Methyl Orange. *J Solid State Chem* 2002;165:193–8.
- [7] Li JL, Liu L, Yu Y, Tang YW, Li HL, Du FP. Preparation of highly photocatalytic active nano-size  $\text{TiO}_2\text{--Cu}_2\text{O}$  particle composites with a novel electrochemical method. *Electrochem Commun* 2004;6:940–3.
- [8] Bandara J, Hadapangoda CC, Jayasekera WG.  $\text{TiO}_2/\text{MgO}$  composite photocatalyst: the role of MgO in photoinduced charge carrier separation. *Appl Catal B Environ* 2004;50:83–8.
- [9] Li XZ, Li FB, Yang CL, Ge WK. Photocatalytic activity of  $\text{WO}_x\text{--TiO}_2$  under visible light irradiation. *J Photochem Photobiol A Chem* 2001;141:209–17.
- [10] Shchukin D, Poznyak S, Kulak A, Pichat P.  $\text{TiO}_2\text{--In}_2\text{O}_3$  photocatalysts: preparation, characterizations and activity for 2-chlorophenol degradation in water. *J Photochem Photobiol A Chem* 2004;162:423–30.
- [11] Marci G, Augugliaro V, Lo'pez-Munoz MJ, Martín C, Palmisano L, Rives V, et al. Preparation, characterization and photocatalytic activity of polycrystalline  $\text{ZnO}/\text{TiO}_2$  systems. 2. Surface, bulk characterization, 4-nitrophenol photodegradation in liquid–solid regime. *J Phys Chem B* 2001;105:1033–40.
- [12] Takahashi YK, Ngaotrakanwivat P, Tsuma T. Energy storage  $\text{TiO}_2\text{--MoO}_3$  photocatalysts. *Electrochim Acta* 2004;49:2025–9.
- [13] Wu L, Yu JC, Fu XZ. Characterization and photocatalytic mechanism of nanosized CdS coupled  $\text{TiO}_2$  nanocrystals under visible light irradiation. *J Mol Catal A Chem* 2006;244:25–32.
- [14] Su H, Xie Y, Gao P, Xiong Y, Qian Y. Synthesis of  $\text{MS}/\text{TiO}_2$  ( $\text{M} = \text{Pb}, \text{Zn}, \text{Cd}$ ) nanocomposites through a mild sol–gel process. *J Mater Chem* 2001;11:684–6.
- [15] Chatterjee D, Dasgupta S, Rao NN. Visible light assisted photodegradation of halocarbons on the dye modified  $\text{TiO}_2$  surface using visible light. *Sol Energy Mater Sol Cells* 2006;90:1013–20.
- [16] Jing LQ, Qun YC, Wang BQ, Li SD, Jiang BJ, Yang LB, et al. Review of photoluminescence performance of nano-sized semiconductor materials and its relationships with photocatalytic activity. *Sol Energy Mater Sol Cells* 2006;90:1773–87.
- [17] Muruganandham M, Sobana N, Swaminathan M. Solar assisted photocatalytic and photochemical degradation of Reactive Black 5. *J Hazard Mater B* 2006;137:1371–6.
- [18] Muruganandham M, Swaminathan M. Solar photocatalytic degradation of a reactive azo dye in  $\text{TiO}_2$ -suspension. *Sol Energy Mater Sol Cells* 2004;81:439–57.
- [19] Wang C, Xu BQ, Wang XM, Zhao JC. Preparation and photocatalytic activity of  $\text{ZnO}/\text{TiO}_2/\text{SnO}_2$  mixture. *J Solid State Chem* 2005;178:3500–6.
- [20] Gouvea K, Wypych F, Moraes SG, Duran N, Nagata N, Peralta-Zamora P. Semiconductor-assisted photocatalytic degradation of reactive dyes in aqueous solution. *Chemosphere* 2000;40:433–40.
- [21] Dindar S, Icli J. Unusual photoreactivity of zinc oxide irradiated by concentrated sunlight. *J Photochem Photobiol A Chem* 2001;140:263–8.
- [22] Behnajady MA, Modirshahla N, Hamzavi R. Kinetic study on photocatalytic degradation of C.I. Acid Yellow 23 by  $\text{ZnO}$  photocatalyst. *J Hazard Mater B* 2006;133:226–32.
- [23] Addamo M, Augugliaro V, Paola AD, García-López E, Loddo V, Marci G, et al. Preparation, characterization, photoactivity of polycrystalline nanostructured  $\text{TiO}_2$  catalysts. *J Phys Chem B* 2004;108:3303–10.
- [24] Serpone N, Maruthamuthu P, Pichat P, Pelizzetti E, Hidaka H. Exploiting the interparticle electron transfer process in the photocatalysed oxidation of phenol, 2-chlorophenol and pentachlorophenol: chemical evidence for electron and hole transfer between coupled semiconductors. *J. Photochem Photobiol A Chem* 1995;85:247–55.
- [25] Sukharev V, Kershaw R. Concerning the role of oxygen in photocatalytic decomposition of salicylic acid in water. *J Photochem Photobiol A Chem* 1996;98:165–9.
- [26] Kim DS, Park YS. Photocatalytic decolorization of Rhodamine B by immobilized  $\text{TiO}_2$  onto silicone sealant. *Chem Eng J* 2006;116:133–7.
- [27] Bizani E, Fytianos K, Poullos I, Tsiridis V. Photocatalytic decolorization and degradation of dye solutions and wastewaters in the presence of titanium dioxide. *J Hazard Mater* 2006;136:85–94.
- [28] Shimizu N, Ogino C, Dadjour MF, Murata T. Sonocatalytic degradation of Methylene Blue with  $\text{TiO}_2$  pellets in water. *Ultrason Sonochem* 2007;14:184–90.
- [29] Chen CC. Degradation pathways of Ethyl Violet by photocatalytic reaction with  $\text{ZnO}$  dispersions. *J Mol Catal A Chem* 2006;264:82–92.
- [30] Muruganandham M, Swaminathan M. Photocatalytic decolourisation and degradation of Reactive Orange 4 by  $\text{TiO}_2\text{--UV}$  process. *Dyes Pigments* 2006;68:133–42.
- [31] Akyol A, Yatmaz HC, Bayramoglu M. Photocatalytic decolorization of Remazol Red RR in aqueous  $\text{ZnO}$  suspensions. *Appl Catal B Environ* 2004;54:19–24.
- [32] Sahoo C, Gupta AK, Pal Anjali. Photocatalytic degradation of Methyl Red dye in aqueous solutions under UV irradiation using  $\text{Ag}^+$  doped  $\text{TiO}_2$ . *Desalination* 2005;181:91–100.
- [33] Zhang RB, Gao L, Zhang QH. Photodegradation of surfactants on the nanosized  $\text{TiO}_2$  prepared by hydrolysis of the alkoxide titanium. *Chemosphere* 2004;54:405–11.